Coherent wave transmission in quasi-one-dimensional systems with Lévy disorder

Ilias Amanatidis
Center for Theoretical Physics of Complex Systems, Institute for Basic Science, Daejeon 34051, Republic of Korea

Ioannis Kleftogiannis*
Department of Physics, National Taiwan University, Taipei 10617, Taiwan

Fernando Falceto and Víctor A. Gopar
Departamento de Física Teórica and BIFI, Universidad de Zaragoza, Pedro Cerbuna 12, 50009 Zaragoza, Spain
(Received 28 September 2017; published 26 December 2017)

We study the random fluctuations of the transmission in disordered quasi-one-dimensional systems such as disordered waveguides and/or quantum wires whose random configurations of disorder are characterized by density distributions with a long tail known as Lévy distributions. The presence of Lévy disorder leads to large fluctuations of the transmission and anomalous localization, in relation to the standard exponential localization (Anderson localization). We calculate the complete distribution of the transmission fluctuations for a different number of transmission channels in the presence and absence of time-reversal symmetry. Significant differences in the transmission statistics between disordered systems with Anderson and anomalous localizations are revealed. The theoretical predictions are independently confirmed by tight-binding numerical simulations.

DOI: 10.1103/PhysRevE.96.062141

I. INTRODUCTION

Coherent wave-interference phenomena have been experimentally and theoretically investigated in different complex systems such as disordered waveguides, photonic crystals, cold atoms, and disordered quantum wires. One of the most celebrated effects of waves in random media is the Anderson localization: an exponential decay in space produced by destructive interference. The phenomenon of Anderson localization was originally predicted for electrons [1], but being fundamentally a wave phenomenon, Anderson localization has been observed also in electromagnetic and acoustic experiments, Bose-Einstein condensates, and entangled photons (see, for instance, [2–12]).

Wave scattering in complex media has been widely investigated within different approaches. In particular, the so-called Dorokhov-Mello-Pereyra-Kumar (DMPK) equation [13] has been successfully applied to study several statistical properties of electronic transport through disordered quantum wires, as well as classical waves in disordered structures. The DMPK equation is a diffusion equation that describes the evolution of the probability density of the transmission eigenvalues as a function of the length of the system. Remarkably, within this approach, the statistical properties of the transmission depend only on a few physical parameters of the system such as the localization length and the presence (or absence) of time-reversal symmetry, i.e., all other details of the system are irrelevant for the statistical description of the transport.

The diffusion approach to wave transport (the DMPK equation) has been applied to study different statistical properties of functions of the transmission [13,14] in systems where quantum wave functions (electrons) or classical electromagnetic waves are exponentially localized in space (Anderson localization). The presence of disorder, however, does not necessarily lead to the standard Anderson localization. Actually, nonstandard localization can be produced by different means in random media. For instance, it has been shown that electrons in disordered quantum wires at the band center [15–17] and armchair graphene disordered nanoribbons [18] are anomalously localized. In particular, it has been experimentally and theoretically shown that random configurations of the disorder characterized by probability densities with a power-law tail (also known as Lévy distributions) produce anomalous localization, i.e., waves are more weakly localized in space in relation to the standard Anderson localization. For experimental realizations of Lévy disorder, see, for instance, Refs. [19,20]. Those works, however, were restricted to one-dimensional systems or structures where only a single transmission eigenvalue or transmission channel is relevant. It is also worth mentioning that Lévy-type distributions have been used to study different problems in a wide range of science disciplines [21–28].

In general, however, the transmission through a system is given by the contribution of several transverse modes or transmission channels [Eq. (14)]. Therefore, it is highly desirable to go beyond the single-channel case and consider the possibility that several transmission channels contribute to the transport, which is also a less restrictive condition from an experimental point of view. Additionally, the multichannel case allows us to study the effect of the absence (or presence) of time-reversal symmetry in Levy disordered systems.

With the above motivation, in this work we extend the diffusion approach to consider the case of anomalous localization in quasi-one-dimensional (quasi-1D) disordered systems, where several transmission channels play a role, i.e., we study the statistical properties of the transmission of waves that are anomalously localized in relation to those with standard Anderson localization. In order to induce anomalous localization, we will consider that the random configurations of the scatterers in a quasi-1D disordered system follow a

*Present address: Physics Division, National Center for Theoretical Sciences, Hsinchu 300, Taiwan.

distribution with a long tail: If x is a random variable with probability density $\rho(x)$, then for large x, $\rho(x) \sim 1/x^{1+\alpha}$ with $0 < \alpha < 2$. This kind of distribution is also known as a Lévy-type distribution or an α-stable distribution [29–31]. We notice that for $0 < \alpha < 1$, the first moment of $\rho(x)$ diverges. In this work we will consider the range $0 < \alpha < 1$, where the effects of Lévy disorder are strong, as we will show.[1]

The present work is an extension of the one-dimensional case studied in Ref. [32] to the multichannel case. This extension allows us to investigate the transport properties of the transmission under physical conditions that cannot be considered in the 1D case such as the effects of breaking the time-reversal symmetry of the system. All our theoretical predictions are independently confirmed by numerical simulations of quasi-one-dimensional disordered systems using a tight-binding model.

The remainder of this paper is organized as follows. For the sake of completeness, the next section is devoted to the problem of transport in 1D disordered systems or a single transmission channel. Both standard and anomalous localizations are studied and some previous results of Ref. [32] are reproduced. In Sec. III we extend our results to the multichannel transmission case. We briefly introduce some elements of the DMPK equation whose solution gives the joint probability density function of N transmission channels, which is used later to calculate the transmission distribution in the presence of Lévy disorder for systems supporting an arbitrary number of channels. Several examples of the transmission distribution for Lévy disordered systems are shown for systems which preserve or break time-reversal symmetry. In Sec. IV we give a summary and the conclusions of our work.

II. SINGLE TRANSMISSION CHANNEL

Disordered systems with Lévy-type disorder[2] and a single transmission channel were studied in Ref. [32]. Here we briefly present this case for the sake of completeness and since it is used to derive the length dependence of the multichannel transmission, as we show below.

Thus, following Ref. [32], we consider a one-dimensional disordered system with scatterers randomly placed along its length L. The key ingredient in this model is that the random distance between the scatterers follows a distribution with a long tail. To obtain the statistical properties of the transmission in the presence of Lévy-type disorder, we extend the results of random-matrix calculations for standard disordered systems.

A. Standard localization

As previously mentioned, the scaling approach to localization and random-matrix theory has been extensively developed in the past [13,14,37] and applied to describe the statistical properties of transport in standard disordered media, i.e., systems whose disorder models involve distributions with finite mean values. Within the scaling theory framework, a diffusion-type equation for the probability distribution of the transmission T was derived and conveniently written in terms of the variable λ as [38]

$$l\frac{\partial p_s(\lambda)}{\partial L} = \frac{\partial}{\partial \lambda}\left[\lambda(\lambda+1)\frac{\partial p_s(\lambda)}{\partial \lambda}\right], \tag{1}$$

where $\lambda = 1/(1+T)$. The solution of Eq. (1) can be written as [39]

$$p_s(T) = \frac{s^{-3/2}}{\sqrt{2\pi}}\frac{e^{-s/4}}{T^2}\int_{y_0}^{\infty} dy\, \frac{y e^{-y^2/4s}}{\sqrt{\cosh y + 1 - 2/T}}, \tag{2}$$

where $y_0 = \operatorname{arcosh}(2/T - 1)$ and $s = L/l$. We point out that the distribution of the transmission is determined by a single microscopic property of the system: the mean free path l, in $s = L/l$.

From the distribution $p_s(T)$ we can obtain any average value of the transmission. In particular, an exponential decay of the average transmission with the length is found,

$$\langle T\rangle \propto \exp(-L/2l), \tag{3}$$

while the average of the logarithm of the transmission is given by

$$\langle -\ln T\rangle = L/l. \tag{4}$$

We notice that the mean free path can thus be obtained from $\langle -\ln T\rangle$. For later purposes, at this point we also remark that $\langle -\ln T\rangle$ is a linear function of L.

Let us illustrate the above results [Eqs. (2)–(4)]. This will be useful for contrasting the effects of anomalous localization due to the presence of Lévy-type disorder in the next section.

Figure 1(a) shows the linear (main frame) and exponential decay (inset) behavior of the averages $\langle -\ln T\rangle$ and $\langle T\rangle$ in Eqs. (3) and (4), respectively. The results of numerical simulations (circles), using a tight-binding model (see the Appendix), are in agreement with the theoretical results (solid lines). In Fig. 1(b) we show the transmission distribution (solid line) as given in Eq. (2) for $s = 0.93$, with the histogram corresponding to the transmission distribution obtained from the tight-binding simulations (see the Appendix). Thus, we can observe that Eq. (2) and the numerical simulations are in good agreement.

B. Anomalous localization

We now introduce a Lévy-type model for the disorder that leads to anomalous localization. Following Ref. [32], we consider that ν scatterers are randomly distributed in a system of length L and assume that their separation x follows a probability density with a long tail

$$\rho(x) \sim \frac{c}{x^{1+\alpha}} \tag{5}$$

for large x. Here c is a constant. As we already mentioned, the first moment of $\rho(x)$ diverges, which implies that the mean free path l diverges. We recall that l governs the statistics of the transmission in the standard localization problem, as pointed out in the preceding section. Therefore, we might

[1] One can extend the present model to the case $1 < \alpha < 2$; however, we restrict ourselves to $0 < \alpha < 1$, where the effects of anomalous localization are stronger.

[2] For 1D systems with Lévy disorder in the incoherent regime, see, for instance, Refs. [33–36].

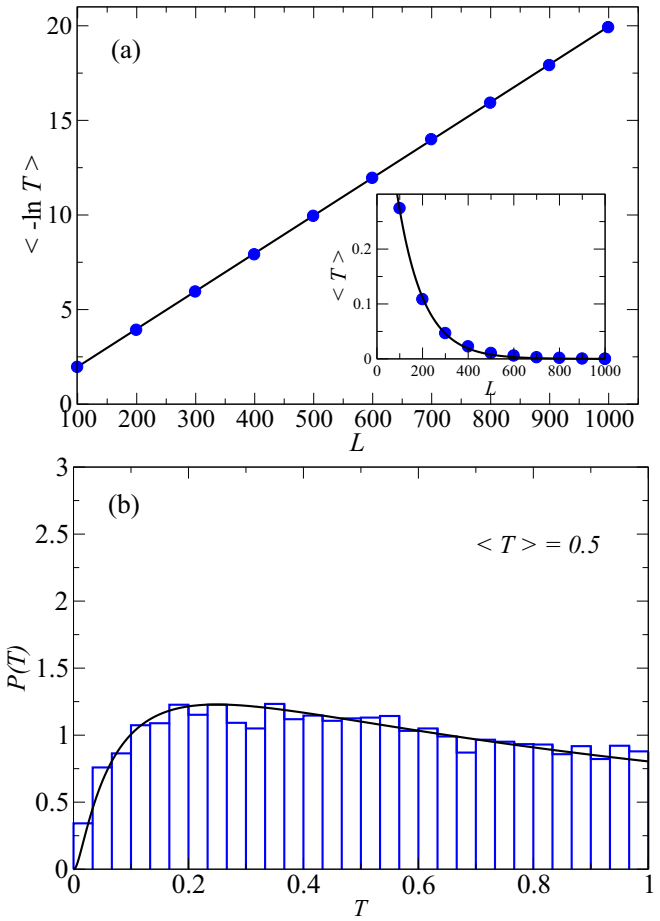

FIG. 1. Transmission results for 1D systems with standard localization. (a) Linear (main frame) and exponential (inset) dependence of $\langle \ln T \rangle$ and $\langle T \rangle$, respectively, with the system length L. The solid lines correspond to the theoretical results, while the closed circles are obtained from the numerical simulations. (b) Complete distribution of the transmission $P(T)$ for a standard disordered system with average $\langle T \rangle = 0.5$. The solid line corresponds to the theoretical distribution, while the histogram is extracted from the numerical simulations.

expect a nonstandard behavior of the transmission statistics in the presence of Lévy disorder.

Let us define the probability density $\Pi_L(\nu)$ of the number of scatterers in a system of length L. It has been shown [32] that $\Pi_L(\nu)$ is given in terms of the probability density distribution $q_{\alpha,c}(x)$ of the Lévy distribution as

$$\Pi_L(\nu) = \frac{2}{\alpha} \frac{L}{(2\nu)^{(1+\alpha)/\alpha}} q_{\alpha,c}(L/(2\nu)^{1/\alpha}) \tag{6}$$

for $0 < \alpha < 1$, in the limit $L \gg c^{1/\alpha}$. We remark that $q_{\alpha,c}(x)$ has a power-law tail[3] $q_{\alpha,c}(x) \sim c/x^{1+\alpha}$ for large values of x.

We now introduce the average values $\langle \ln T \rangle_\nu$ and $\langle \ln T \rangle_L$ for systems with a fixed number of scatterers ν and fixed length L, respectively. From the standard scaling theory of localization summarized in preceding section, $\langle -\ln T \rangle_\nu$ is proportional to ν: $\langle -\ln T \rangle_\nu = a\nu$, a being a constant [40]. Hence, we have that

$$\langle -\ln T \rangle_L = \int_0^\infty \langle -\ln T \rangle_\nu \Pi_L(\nu) d\nu \tag{7}$$

$$= \int_0^\infty a\nu \frac{2}{\alpha} \frac{L}{(2\nu)^{(1+\alpha/)\alpha}} q_{\alpha,c}(L/(2\nu)^{1/\alpha}) d\nu, \tag{8}$$

where we have substituted Eq. (6). Using the scaling property of the Lévy distributions $c^{1/\alpha} q_{\alpha,c}(c^{1/\alpha}x) = q_{\alpha,1}(x)$ and introducing the variable $z = L/(2c\nu)^{1/\alpha}$, we obtain

$$\langle -\ln T \rangle_L = L^\alpha \frac{a}{c} \frac{1}{2} \int_0^\infty z^{-\alpha} q_{\alpha,1}(z) dz = L^\alpha \frac{a}{c} I_\alpha, \tag{9}$$

where $I_\alpha = (1/2)\int_0^\infty z^{-\alpha} q_{\alpha,1}(z) dz = \cos(\pi\alpha/2)/2\Gamma(1+\alpha)$ [41], with Γ the Gamma function. We point out that Eq. (9) shows a nonstandard behavior

$$\langle -\ln T \rangle_L \propto L^\alpha, \tag{10}$$

i.e., $\langle -\ln T \rangle_L$ is a power function of L, in contrast to the linear behavior with L expected in the usual scaling theory [see Eq. (4)]. Similarly, the average of the transmission decays with the length as

$$\langle T \rangle_L \sim 1/L^\alpha, \tag{11}$$

which is also in contrast to the expected exponential decay in one dimension [see Eq. (3)].

In Figs. 2(a) and 2(b) we have verified the above results [Eqs. (11) and (10)] for $\alpha = 1/2$ by comparing with numerical simulations. As it was predicted, $\langle \ln T \rangle$ has a power-law behavior with L, in this case with power $\alpha = 1/2$, while $\langle T \rangle$ decays as $L^{-1/2}$.

We now calculate the complete distribution of the transmission $P_\mu(T)$ for fixed length L in the presence of Lévy disorder, here $\langle -\ln T \rangle_L = \mu$. The distribution $P_\mu(T)$ can be obtained from $p_s(T)$ [Eq. (2)] using that in the standard diffusion approach the parameter s is proportional to the number of scatterers ν, i.e., $s = a\nu$, a being a constant. Thus, we introduce the information of the Lévy disorder through the distribution $\Pi_L(\nu)$ in Eq. (6) to obtain that the probability density of the transmission $P_\mu(T)$ is given by

$$P_\mu(T) = \int_0^\infty p_{a\nu}(T) \Pi_L(\nu) d\nu. \tag{12}$$

Using Eqs. (6) and (9) as well as the scaling properties of the Lévy distributions, we finally have that

$$P_\mu(T) = \int_0^\infty p_{s(\alpha,\mu,z)}(T) q_{\alpha,1}(z) dz, \tag{13}$$

where we have defined $s(\alpha,\mu,z) = \mu/2z^\alpha I_\alpha$. We remark that the distribution $P_\mu(T)$ in Eq. (13) depends only on two parameters $\langle -\ln T \rangle_L = \mu$ and α, i.e., other details of the disorder configurations are irrelevant.

As an example, in Fig. 2(b) we show the complete transmission distribution for a disordered system with $\langle T \rangle = 0.5$ and $\alpha = 1/2$. It is interesting to compare the distribution of the transmission for both standard and anomalous localizations

[3]The explicit expression for the probability density $q_{\alpha,c}(x)$ is more conveniently written using the Fourier transform $\hat{q}_{\alpha,c}(k) = \exp\{-|k|^\alpha [A\theta(k) + A^*\theta(-k)]\}$, where θ is the Heaviside step function and $A = -c\Gamma(-\alpha)e^{i(\pi\alpha/2)}$, Γ being the Gamma function.

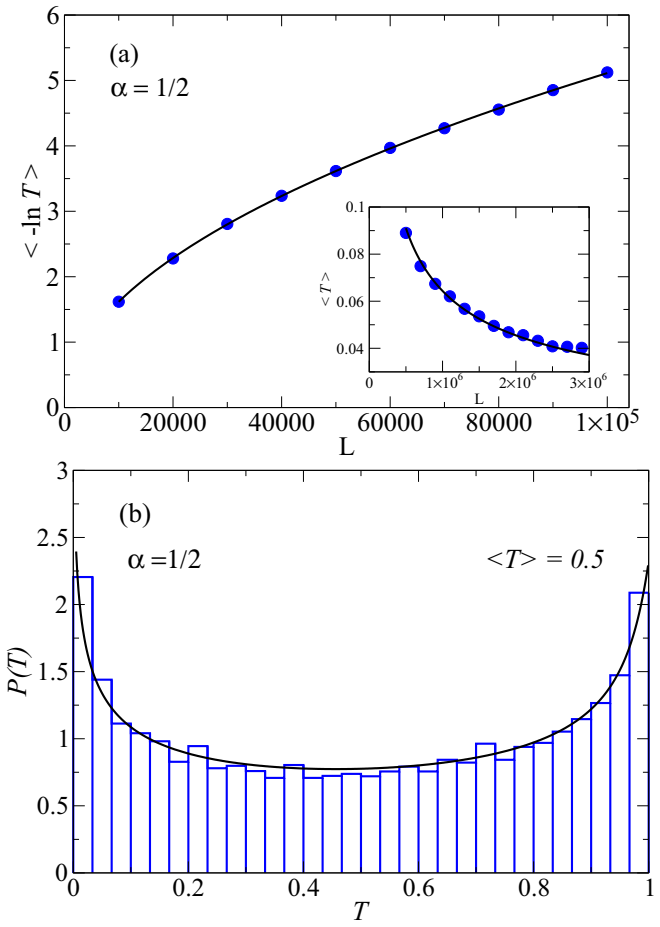

FIG. 2. Transmission results for systems with Lévy disorder ($\alpha = 1/2$). (a) Power-law dependence of $\langle \ln T \rangle$ (main frame) and $\langle T \rangle$ (inset) for a 1D system with Lévy disorder with $\alpha = 1/2$. See Eqs. (10) and (11). Closed circles correspond to the numerical simulation results. (b) Complete distribution $P(T)$ for a Lévy disordered system with $\alpha = 1/2$ and $\langle T \rangle = 0.5$. The solid line is obtained from Eq. (13), while the histogram is obtained from the numerical simulations.

[Figs. 1(b) and 2(b), respectively]. Notice that both distributions are obtained for disordered systems with $\langle T \rangle = 0.5$, however, the shapes of the distributions are totally different. In particular, in the case of anomalous localization, the transmission distribution show two peaks at $T = 0$ and $T = 1$, which is a consequence of the stronger random fluctuations of the transmissions in the presence of Lévy-type disorder.

III. MULTICHANNEL TRANSMISSION

In the preceding section we considered the simplest case of 1D disordered systems where only a single transmission channel plays a role. We now extend our analysis to a more general case where the total transmission is given by the contribution of several transmission channels. Additionally, by considering the multichannel case we can study the effects of the presence, or absence, of time-reversal symmetry. We will present particular cases of two and three transmission channels to illustrate our results. Similarly to Sec. II, we first give a summary of the random-matrix theory for standard disorder and later we extend the results to consider Lévy-type disorder.

A. Standard localization

Let us consider a disordered system whose length L is much larger than its width, i.e., a quasi-one-dimensional system. With this geometry, one can neglect diffusion in the transverse direction. Assuming that the system supports N transverse modes, or channels, the total transmission T is given by

$$T = \sum_{n=1}^{N} \tau_n, \tag{14}$$

where τ_n are the eigenvalues of the product $tt^\dagger$, with t the matrix of the transmission amplitudes of a quasi-1D disordered system. Within the diffusion approach [42], the transmission eigenvalues τ_n are random variables whose joint probability distribution function $p(\tau)$ evolves with the system length L according to a Fokker-Planck equation, or DMPK equation, as [13,42]

$$l\frac{\partial p(\lambda)}{\partial L} = \frac{2}{\beta N + 2 - \beta}\frac{1}{J(\lambda)} \times \sum_{i}^{N} \frac{\partial}{\partial \lambda_i}\left[\lambda_i(1+\lambda_i)J(\lambda)\frac{\partial}{\partial \lambda_i}\frac{\partial p(\lambda)}{J(\lambda)}\right], \tag{15}$$

where $\lambda_i = (1-\tau_i)/\tau_i$ and l is the mean free path. The Jacobian $J(\lambda)$ is given by the product $J(\lambda) = \prod_{i<j}^{N} |\lambda_i - \lambda_j|^\beta$. The value of the parameter β depends on the absence ($\beta = 2$) or presence ($\beta = 1$) of time-reversal symmetry. The above diffusion equation (15) is a generalization of the single-channel case in Eq. (1). We also notice that the mean free path l is the only microscopic information that enters the diffusion equation, as in the single-transmission-channel problem in the preceding section.

On the other hand, an analytical expression for the solution of the DMPK equation (15) for both unitary ($\beta = 1$) and orthogonal ($\beta = 2$) symmetries has been obtained in the metallic and insulating regimes [43], which also has been useful to study statistical properties of the transmission in the metal-insulating crossover regime [44,45]. This solution can be written as

$$p_s^{(\beta)}(\lambda) = \frac{1}{Z}\exp[-\beta H(\lambda)], \tag{16}$$

where $Z = \int \exp[-\beta H(\lambda)]\Pi_i d\lambda_i$ and

$$H(\lambda) = \sum_{i<j}^{N} u(\lambda_i,\lambda_j) + \sum_{i}^{N} V(\lambda_i). \tag{17}$$

The functions $u(\lambda_i,\lambda_j)$ and $V(\lambda_i)$ are more conveniently written in terms of the variables x_i, where $\lambda_i = \sinh^2 x_i$ as

$$u(x_i,x_j) = -\frac{1}{2}\left[\ln|\sinh^2 x_i - \sinh^2 x_j| - \ln\left|x_i^2 - x_j^2\right|\right],$$
$$V(x_i) = \frac{l(\beta N + 2 - \beta)}{2L\beta}x_i^2 - \frac{1}{2\beta}\ln|x_i \sinh 2x_i|. \tag{18}$$

Therefore, using the joint probability distribution given in Eq. (16), the distribution of the transmission is given by the average

$$p_s^{(\beta)}(T) = \left\langle \delta\left(T - \sum_i^N \frac{1}{1+\lambda_i} \right) \right\rangle, \tag{19}$$

where, as previously defined, s is the length of the system in units of the mean free path ($s = L/l$) and the angular brackets denote the average performed with the joint probability distribution $p_s^{(\beta)}(\lambda)$ [Eq. (16)].

As we have mentioned, the above diffusion approach has been successfully verified in a number of numerical and experimental works where Anderson localization is present [13,14]. With the above results, we are now ready to introduce Lévy-type disorder in a multichannel disordered media.

B. Anomalous localization

Let us assume the presence of Lévy-type disorder, as described in Sec. II B, in a multichannel system of length L. In addition to the interest in studying the transmission properties of Lévy-type disorder media supporting many channels, the multichannel problem adds the possibility of studying the effects of breaking the time-reversal symmetry of the system, characterized by the parameter β. We will consider the cases of $\beta = 1$ (preserved time-reversal symmetry) and $\beta = 2$ (broken time-reversal symmetry).

The distribution of the transmission for Lévy-type disordered systems in the multichannel case can be obtained by following the steps of the one-channel case in Sec. II B. Although the generalization to the multichannel case is straightforward, the calculations are more involved and no simple analytical relations have been obtained.

As in the one-channel case, the transmission distribution for multichannel Lévy disordered systems can be obtained once the probability density of the number of scatterers in a system of fixed length L is known, assuming the separation between scatterers follows a Lévy-type distribution. This probability density was already obtained in Sec. II B, Eq. (6). Therefore, with the knowledge of the transmission distribution from the standard random-matrix theory given by Eq. (19), we write the density probability distribution of the transmission for Lévy-type disorder as

$$P_\mu^{(\beta)}(T) = \int_0^\infty p^{(\beta)}_{s(\alpha,\mu,N,z)}(T) q_{\alpha,1}(z) dz, \tag{20}$$

where the distribution $p^{(\beta)}_{s(\alpha,\mu,N,z)}(T)$ is given in Eq. (19) with s replaced by a function $s(\alpha,\mu,N,z)$ and $\mu = \langle \ln T \rangle_L$. For the single transmission channel, we have given an expression for $s(\alpha,\mu,N=1,z)$ in terms of the average $\langle \ln T \rangle_L$ since $s = \langle \ln T \rangle$ in the case of standard disorder. In the multichannel case, however, we cannot derive an analytical expression for $s(\alpha,\mu,N,z)$ since there is no general expression between s and $\langle \ln T \rangle_L$ for an arbitrary number of channels. For $N \gg 1$, however, $\langle \ln T \rangle \approx L/\beta N l = s/\beta N$. Thus, in this limit, we can write $s(\alpha,\mu,N,z) = \beta N \mu / 2 z^\alpha I_\alpha$. To overcome this problem for an arbitrary number of channels, we consider that the function $s(\alpha,\mu,N,z)$ is of the form b/z^α, where b is a constant whose value is fixed to the one that reproduces the numerical value of the average $\langle T \rangle_L$ or, equivalently, $\langle \ln T \rangle_L$.

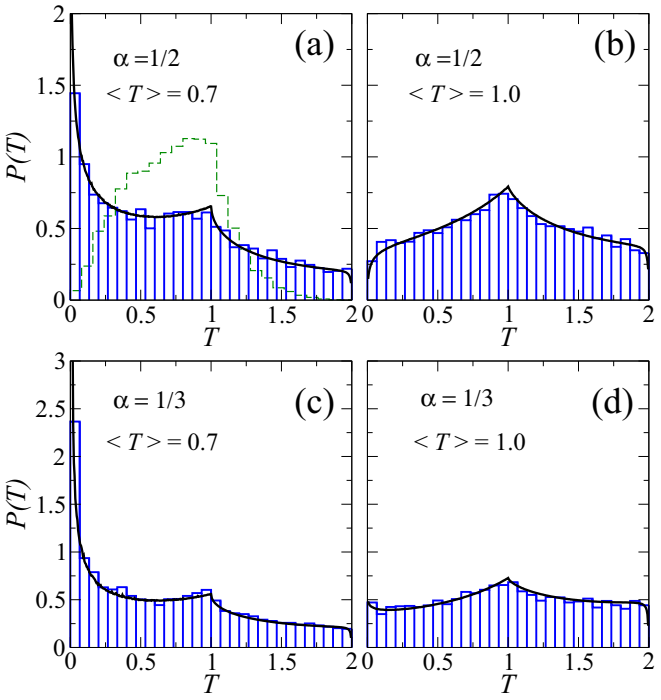

FIG. 3. Transmission distribution for $N = 2$ transmission channels with Lévy disorder characterized by (a) and (b) $\alpha = 1/2$ and (c) and (d) $\alpha = 1/3$. The solid lines are obtained according to the theory described in the main text, while the histograms are extracted from the tight-binding numerical simulations. The values of the standard deviation δT and the constant b in $s(\alpha,\mu,N,z)$ are (a) $\delta T = 0.54$ and $b = 2.5$, (b) $\delta T = 0.52$ and $b = 1.35$, (c) $\delta T = 0.56$ and $b = 2.6$, and (d) $\delta T = 0.54$ and $b = 1.2$. Good agreement between theory and numerical simulation can be seen in all panels. For comparison with Lévy disordered systems, (a) shows $P(T)$ (green-dashed-line histogram) for systems with standard disorder and ensemble average $\langle T \rangle = 0.7$.

We thus now present several examples of the transmission distribution as given by Eq. (20) for $N = 2$ and 3 transmission channels and different values of the power decay α, in the presence and absence of time-reversal symmetry. The theoretical results are obtained by numerical integration of Eq. (20). In all cases, our results are independently verified by tight-binding numerical simulations. Additionally, in order to contrast and compare the transmission statistics of standard and Lévy disordered systems, in Figs. 3(a), 4(a), 5(a), and 6(a) we include the transmission distribution expected for the cases of standard disordered systems.

1. Preserved time-reversal symmetry

We first assume that time-reversal symmetry is present in the system, i.e., we consider the symmetry class $\beta = 1$ and, as it was previously mentioned, we will concentrate on the cases of $N = 2$ and 3 channels. The distribution of the transmission for two channels is shown in Fig. 3 for two different values of the average $\langle T \rangle$ and disorder configurations characterized by the decay power $\alpha = 1/2$ and $1/3$. The histograms (blue

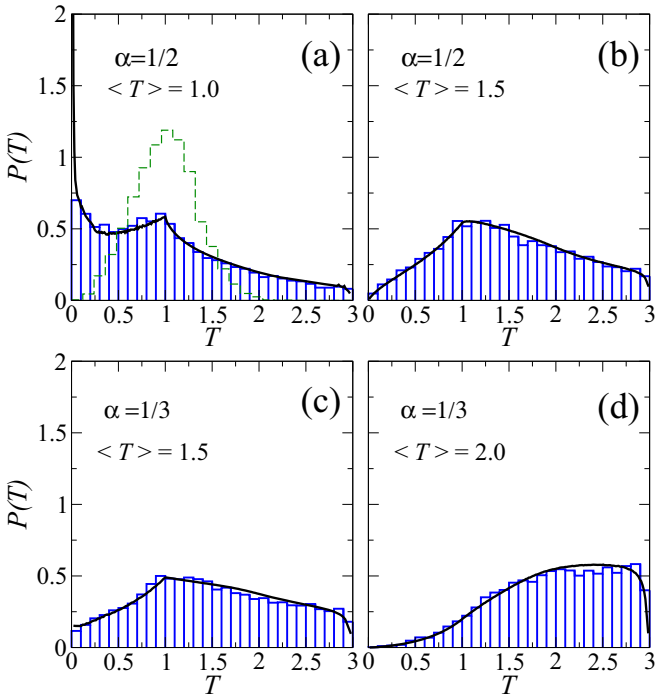

FIG. 4. Transmission distribution $P(T)$ for $N = 3$ transmission channels with Lévy disorder characterized by (a) and (b) $\alpha = 1/2$ and (c) and (d) $\alpha = 1/3$. The solid lines are obtained according to the theory described in the main text, while the histograms are extracted from the tight-binding numerical simulations. The values of the standard deviation δT and the constant b in $s(\alpha,\mu,N,z)$ are (a) $\delta T = 0.73$ and $b = 2.8$, (b) $\delta T = 0.70$ and $b = 1.36$, (c) $\delta T = 0.75$ and $b = 2.6$, and (d) $\delta T = 0.62$ and $b = 0.5$. Good agreement between theory and numerical simulation can be seen in all panels. The (green-dashed-line) histogram in (a) shows the distribution $P(T)$ for systems with standard disorder with ensemble average $\langle T\rangle = 1.0$.

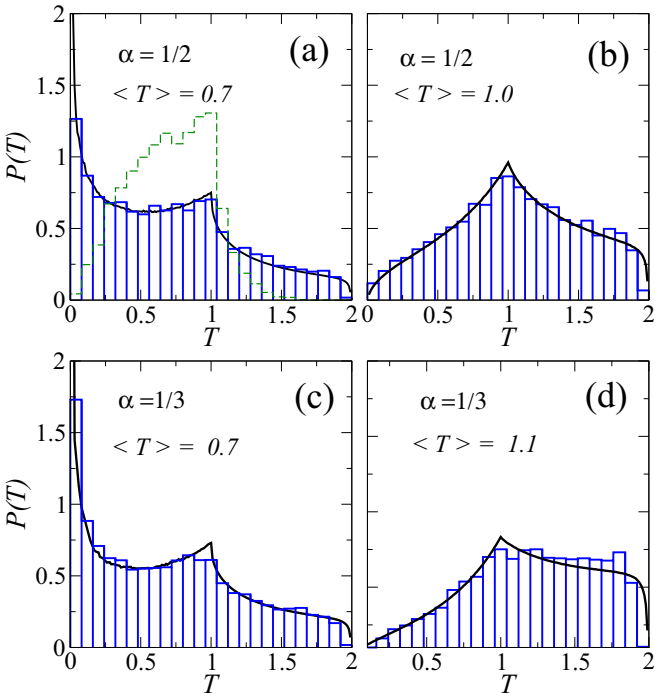

FIG. 5. Applied magnetic field ($\phi = 0.15$). Transmission distribution $P(T)$ with broken time-reversal symmetry for $N = 2$ transmission channels with Lévy disorder characterized by (a) and (b) $\alpha = 1/2$ and (c) and (d) $\alpha = 1/3$. The solid lines are obtained according to the theory described in the main text, while the histograms are extracted from the tight-binding numerical simulations. The values of the standard deviation δT and the constant b in $s(\alpha,\mu,N,z)$ are (a) $\delta T = 0.5$ and $b = 3.3$, (b) $\delta T = 0.46$ and $b = 1.3$, (c) $\delta T = 0.52$ and $b = 2.5$, and (d) $\delta T = 0.46$ and $b = 0.8$. Theory and numerical simulations are in agreement in all panels. The (green-dashed-line) histogram in (a) shows the distribution $P(T)$ for systems with standard disorder and broken time-reversal symmetry with ensemble average $\langle T\rangle = 0.7$.

solid line) in Fig. 3 are obtained by tight-binding numerical simulations (see the Appendix) by collecting the transmission data from 10 000 disorder configurations, while the theoretical predictions (black solid lines) are calculated according to Eq. (20) with $p_{s(\alpha,\mu,N,z)}(T)$ given by Eq. (19) with $N = 2$ and $\beta = 1$.

The distributions in Figs. 3(a) and 3(b) correspond to the case of $\alpha = 1/2$ with average transmissions $\langle T\rangle = 0.7$ and 1.0, respectively. Similarly, Figs. 3(c) and 3(d) show the transmission distribution for $\alpha = 1/3$. We can observe good agreement between theoretical (solid lines) and numerical simulation results (histograms) in all cases.

It is expected that the fluctuations of the transmission become large as the power exponent α decreases. This implies that the transmission distributions for $\alpha = 1/3$ are wider than those for $\alpha = 1/2$. Effectively, for a fixed value of the $\langle T\rangle$, the value of the standard deviation $\delta T = \sqrt{\langle T^2\rangle - \langle T\rangle^2}$ for systems with $\alpha = 1/3$ is larger than those with $\alpha = 1/2$ (see the caption of Fig. 3), although for the particular cases shown in Figs. 3(a) and 3(c), as well as in Figs. 3(b) and 3(d), the difference between the standard deviations is small.

We now consider the case of $N = 3$ transmission channels. Thus, the maximum value of the transmission is 3. In Fig. 4 we show the transmission distribution for $\alpha = 1/2$ and $\alpha = 1/3$ at different transmission averages $\langle T\rangle$. The solid lines are calculated as given by Eq. (20), while the histograms are obtained from the numerical simulations. As in the two-transmission-channel case, disorder configurations with $\alpha = 1/3$ show larger transmission fluctuations than $\alpha = 1/2$. See, for instance, the distributions in Figs. 4(b) and 4(c), which have the same average $\langle T\rangle = 1.5$ but $\delta T = 0.7$ and 0.75, respectively. In all the panels of Fig. 4 good agreement between theory (solid lines) and numerical simulations (histograms) can be seen.

Finally, we remark that the landscapes of the transmission distributions for standard (dashed-line histogram) and Lévy disordered (solid line) systems shown in Fig. 3(a), as well in Fig. 4(a), are quite different. In general, the transmission distributions in the presence of Lévy disorder are wider than the cases in the presence of standard Anderson localization, revealing stronger transmission fluctuations in the former case.

2. *Broken time-reversal symmetry*

We first recall that in the presence of time-reversal symmetry, the reflection probability is slightly higher than the

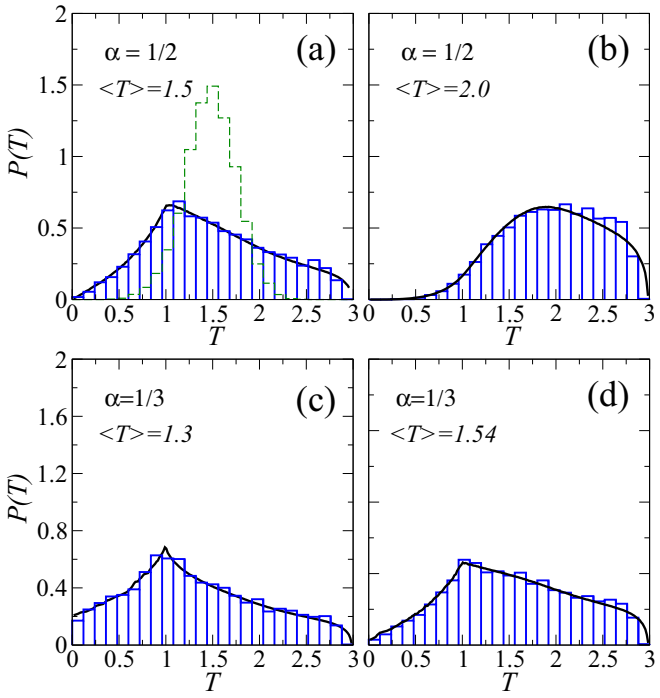

FIG. 6. Applied magnetic field ($\phi = 0.1$). Transmission distribution $P(T)$ with broken time-reversal symmetry for $N = 3$ transmission channels with Lévy disorder characterized by (a) and (b) $\alpha = 1/2$ and (c) and (d) $\alpha = 1/3$. The solid lines are obtained according to the theory described in the main text, while the histograms are extracted from the tight-binding numerical simulations. The values of the standard deviation δT and the constant b in $s(\alpha,\mu,N,z)$ are (a) $\delta T = 0.50$ and $b = 1.6$, (b) $\delta T = 0.51$ and $b = 0.7$, (c) $\delta T = 0.70$ and $b = 1.9$, and (d) $\delta T = 0.67$ and $b = 1.6$. Theory and numerical simulations are in agreement in all panels. The (green-dashed-line) histogram in (a) shows the distribution $P(T)$ for systems with standard disorder and broken time-reversal symmetry with ensemble average $\langle T\rangle = 1.5$.

transmission probability due to constructive interference between two time-reversed scattering processes. This phenomenon is known as weak localization. If time-reversal symmetry is broken, this constructive interference effect is destroyed and the weak localization is suppressed. Therefore, it is expected that the absence of time-reversal symmetry has an effect on the statistics of the transmission.

Let us assume now that we break the time-reversal symmetry of the Lévy disordered systems, i.e., we consider the symmetry class $\beta = 2$. In the numerical simulations, time-reversal symmetry is broken by applying a perpendicular magnetic field to the disordered systems.

In Fig. 5 we show the transmission distribution for $N = 2$ channels with $\alpha = 1/2$ [Figs. 5(a) and 5(b)] and $\alpha = 1/3$ [Figs. 5(c) and 5(d)]. Disordered systems with approximately the same average $\langle T\rangle$ were chosen in Figs. 5(a) and 5(c) [as well as in Figs. 5(b) and 5(d)] for their comparison. Similarly, we show the transmission distributions for $N = 3$ channels with $\alpha = 1/2$ [Figs. 6(a) and 6(b)] and $\alpha = 1/3$ [Figs. 6(c) and 6(d)].

As in the case of preserved time-reversal symmetry in the preceding section, smaller values of α, i.e., a larger tail of the Lévy distribution, lead to stronger transmission fluctuations δT, for a fixed value of the average $\langle T\rangle$. For instance, Figs. 5(a) and 5(c) show a couple of distributions $P(T)$ with $\langle T\rangle = 0.7$, but $\delta T = 0.5$ and 0.52 for $\alpha = 1/2$ and 1/3, respectively.

It is also interesting to compare the transmission distributions in the absence of time-reversal symmetry (Figs. 5 and 6) with those previously shown for the case of preserved time-reversal symmetry (Figs. 3 and 4). As we have mentioned, when time-reversal symmetry is present, constructive interference leads to an enhancement of the reflection. In general, this enhancement is small, but one can observe its effects at the level of the distribution $P(T)$: For instance, at small transmission values (or high reflection), Fig. 3(b) shows that the transmission probability is larger compared to the broken time-reversal symmetry in Fig. 5(b), i.e., reflection is enhanced. This enhancement in the reflection is perhaps better seen by comparing the distributions in Figs. 3(d) and 5(d), although in these figures the average $\langle T\rangle$ is not exactly the same; we can observe that $P(T)$ in Fig. 5(d) is suppressed in the absence of time reversal at small values of T and therefore it is less symmetric with respect to $T = 1$ than $P(T)$ in Fig. 3(d), i.e., reflection processes are promoted when time-reversal symmetry is present.

Finally, we note the strong effect of the presence of Lévy disorder in relation to standard disorder systems. In Figs. 5(a) and 6(a) we have included (green-dashed-line histograms) the transmission distributions for disordered systems with standard Anderson localization, which, as we can see, have a completely different landscape from those of the Lévy disordered systems. In general, the transmission fluctuations are larger in the presence of Lévy disorder and therefore the transmission distributions are wider than in the presence of standard Anderson localization.

IV. CONCLUSION

Most of the research on transport of classical and quantum waves, such as electromagnetic fields and electrons, through random media uses distributions with finite moments to model the disorder in the media. Using these standard disorder models, several theoretical approaches have studied the properties of wave transport, such as the widely known phenomenon of Anderson localization. In particular, a scaling theory of localization has been developed to study the statistical properties of the transport through disordered systems. Within that framework and using random-matrix theory, it has been shown that for one-dimensional and quasi-one-dimensional disordered systems, a single parameter, the localization length, determines the statistical properties of the transmission.

On the other hand, there is a family of probability density functions (Lévy distributions) whose first moment diverges due to their long tails, which are characterized by the exponent α of the power-law tail. Lévy distributions emerge in several and very different phenomena and different areas, such as economy and biology.

In the past [32], we introduced those heavy-tailed distributions to model disorder in random media and study their effects on the transport; however, we restricted ourselves to the case of a single transmission channel. It was found that the statistical properties of the dimensionless conductance (transmission) are

completely determined by two parameters: the power α and the average over disorder realizations $\langle \ln T \rangle$. It was also found that waves become less localized, or anomalously localized, in relation to the case of Anderson localization.

The present work is a generalization of the previous study in Ref. [32] to consider Lévy disordered systems whose total transmission is given by the contribution of several channels. This is also of experimental relevance since it imposes less restrictive conditions than considering systems with a single transmission channel.

Thus, by extending the scaling approach to localization for multichannel standard disordered systems, we have calculated the transmission distribution for multichannel Lévy disordered systems, which is determined by the power α and the average $\langle \ln T \rangle$. We show several examples of the transmission distribution for systems with two and three transmission channels. The theoretical results have been verified by tight-binding numerical simulations. Additionally, we have studied the effects of breaking time-reversal symmetry in the Lévy disordered systems.

We have contrasted the transmission distributions for Lévy and standard disordered systems and showed that the landscape of both distributions is very different. In general, the transmission distributions for Lévy disordered systems are wider, due to the strong random fluctuations of the transmission, than those obtained for standard disordered systems

Finally, we have confirmed all our theoretical results by comparison with tight-binding numerical simulations. Nevertheless, it would be highly desirable to verify experimentally the effects of Lévy disorder on the transport like those we have studied here. For instance, Lévy disorder may be implemented in random microwave-waveguide and/or random optical-fiber experimental setups. Actually, it may be worth remarking that our model does not assume that the microscopic configurations of the disorder follow a Lévy probability distribution, but only that the tail of the density of those disorder configurations has a slow decay, i.e., a power-law tail. Thus, all other details of the disorder are irrelevant for a complete statistical description of the transmission through the macroscopic systems.

ACKNOWLEDGMENTS

We would like to thank X. Ma for bringing Ref. [41] to our attention. V.A.G. acknowledges support from MINECO (Spain) under the Project No. FIS2015-65078-C2-2-P and Subprograma Estatal de Movilidad 2013-2016 under the Project No. PRX16/00166. He is also grateful for the hospitality of the Physics Department of Queens College, The City University of New York, where part of this work was written. F.F. acknowledges support from MINECO (Spain) under the Project No. FPA2015-65745-P and DGA Grant No. 2014-E24/2. The authors gratefully acknowledge the resources from the supercomputer Terminus and technical expertise and assistance provided by the Institute for Biocomputation and Physics of Complex Systems, Universidad de Zaragoza. I.A. acknowledges support provided by the Center for Theoretical Physics of Complex Systems in Daejeon of Korea under Project No. IBS-R024-D1. We also acknowledge support from the National Taiwan University and the Ministry of Science and Technology of Taiwan.

APPENDIX: NUMERICAL SIMULATIONS

In this Appendix we present the numerical model that was used to verify the theoretical predictions of the present work. We consider a standard single-orbital tight-binding square lattice with the Hamiltonian

$$H = \sum_i \epsilon_i c_i^\dagger c_i + \sum_{\langle ij \rangle} (t_{ij} c_i^\dagger c_j + \text{H.c.}), \tag{A1}$$

where ϵ_i is the on-site energy at site i, t_{ij} represents the nearest-neighbor hopping between sites $\langle ij \rangle$, and $c_i^\dagger$ (c_i) is the corresponding creation(annihilation) operator for electrons. For simplicity we set $t_{ij} = t = 1$ and the lattice constant to 1. In this model, the disorder is implemented by random on-site energies ϵ_i, sampled from a uniform distribution in the interval $[-w/2, w/2]$. Throughout this paper, the statistics of the transmission probability are collected from 10 000 different disorder realizations. In order to make the numerical model statistically equivalent to the theoretical model, we consider that the length of the square lattice at each disorder realization is determined by the number of scatterers, whose intermediate spacings are sampled from the Lévy distribution, that can be fitted in a system of length L in the theoretical model.

The transmission probability can be calculated by attaching perfect leads from the left and right, described by Eq. (A1) for $\epsilon_i = 0$, and then applying the Green's-function method [46]. The Green's function is given by

$$G(E) = [EI - H - \Sigma_L(E) - \Sigma_R(E)]^{-1}, \tag{A2}$$

where $\Sigma_{L(R)}(E)$ is the self-energy of the left (right) lead and E is the incident energy of the electrons. The self-energies follow a matrix form

$$\Sigma_{L(R)}(E; n, m) = \sum_{j=1}^{M} \chi_j(n) g(E, j) \chi_j(m), \tag{A3}$$

where M is the number of sites transverse to the transport direction where hard-wall boundary conditions are applied and j is an integer taking values $j = 1, 2, \ldots, M$. We fix the energy at $E = 0.1t$ so that M determines the number of open transmission channels.

The surface Green's function of the square lattice leads $g(E, j)$ at site j is given by [47]

$$g(E, j) = \frac{E - \epsilon(j)}{2} - i\sqrt{1 - \frac{[E - \epsilon(j)]^2}{4}}, \tag{A4}$$

with $\epsilon(j) = 2\cos(\frac{\pi j}{M+1})$ and $|E - \epsilon(j)| < 2$, while $\chi_j(n)$ are the transverse wave functions due to the hard-wall boundary conditions

$$\chi_j(n) = \sqrt{\frac{2}{M+1}} \sin\left(\frac{\pi j n}{M+1}\right), \tag{A5}$$

with $n = 1, \ldots, M$. Then the transmission probability can be calculated by [46]

$$T(E) = \text{Tr}[\Gamma_L(E) G(E) \Gamma_R(E) G(E)^\dagger], \tag{A6}$$

where the matrices $\Gamma_L(E)$ and $\Gamma_R(E)$ are related to the velocities of the incident electrons and can be calculated via

the self-energies from

$$\Gamma_{L(R)}(E) = i[\Sigma_{L(R)} - \Sigma^{\dagger}_{L(R)}]. \tag{A7}$$

Finally, in the case that we break the time-reversal symmetry of the disordered system by applying a magnetic field transverse to the plane of the 2D wire, the tight-binding Hamiltonian for our numerical simulations is given by Eq. (A1), with a modified hopping t_{ij},

$$t_{ij} = e^{i\phi_{ij}}. \tag{A8}$$

The factor ϕ_{ij} is the Peierls phase (see Ref. [47]) between sites i and j given by

$$\phi_{ij} = \frac{2\pi}{\Phi_0}\int_{r_i}^{r_j} \mathbf{A}\, d\mathbf{l}, \tag{A9}$$

where Φ_0 is the flux quantum defined as $\Phi_0 = h/ce$. We assume that the vector potential $\mathbf{A}$ is along the transport direction x, that is, $\mathbf{A} = -By\hat{x}$, corresponding to a homogeneous out-of-plane magnetic field $\mathbf{B} = B\hat{z}$. The phase factor ϕ_{ij} then becomes

$$\phi_{ij} = \frac{2\pi B}{\Phi_0}(x_j - x_i)\Big(\frac{y_j + y_i}{2}\Big), \tag{A10}$$

which is nonzero only for the horizontal hoppings in the square lattice. In all the numerical simulations we measure the magnetic field strength via the flux per square plaquette $\Phi = Ba^2$ in the square lattice, in units of Φ_0.

[1] P. W. Anderson, Phys. Rev. **109**, 1492 (1958).
[2] A. Lagendijk, B. van Tiggelen, and D. S. Wiersma, Phys. Today **62**(8), 24 (2009).
[3] *Fifty Years of Anderson Localization*, edited by E. Abrahams (World Scientific, Singapore, 2010).
[4] G. Roati, C. D'Errico, L. Fallani, M. Fattori, C. Fort, M. Zaccanti, G. Modugno, M. Modugno, and M. Inguscio, Nature (London) **453**, 895 (2008).
[5] A. Crespi, R. Osellame, R. Ramponi, V. Giovannetti, R. Fazio, L. Sansoni, F. De Nicola, F. Sciarrino, and P. Mataloni, Nat. Photon. **7**, 322 (2013).
[6] A. A. Chabanov, M. Stoytchev, and A. Z. Genack, Nature (London) **404**, 850 (2000).
[7] Z. Shi, J. Wang, and A. Z. Genack, Proc. Natl. Acad. Sci. USA **111**, 2926 (2014).
[8] A. Peña, A. Girschik, F. Libisch, S. Rotter, and A. A. Chabanov, Nat. Commun. **5**, 3488 (2014).
[9] A. G. Yamilov, R. Sarma, B. Redding, B. Payne, H. Noh, and H. Cao, Phys. Rev. Lett. **112**, 023904 (2014).
[10] T. R. Kirkpatrick, Phys. Rev. B **31**, 5746 (1985).
[11] H. Hu, A. Strybulevych, J. H. Page, S. E. Skipetrov, and B. A. van Tiggelen, Nat. Phys. **4**, 945 (2008).
[12] L. A. Cobus, S. E. Skipetrov, A. Aubry, B. A. van Tiggelen, A. Derode, and J. H. Page, Phys. Rev. Lett. **116**, 193901 (2016).
[13] P. A. Mello and N. Kumar, *Quantum Transport in Mesoscopic Systems: Complexity and Statistical Fluctuations* (Oxford University Press, Oxford, 2004).
[14] C. W. J. Beenakker, Rev. Mod. Phys. **69**, 731 (1997).
[15] C. M. Soukoulis and E. N. Economou, Phys. Rev. B **24**, 5698 (1981).
[16] S. N. Evangelou and D. E. Katsanos, J. Phys. A: Math. Gen. **36**, 3237 (2003).
[17] I. Amanatidis, I. Kleftogiannis, F. Falceto, and V. A. Gopar, Phys. Rev. B **85**, 235450 (2012).
[18] I. Kleftogiannis, I. Amanatidis, and V. A. Gopar, Phys. Rev. B **88**, 205414 (2013).
[19] P. Barthelemy, J. Bertolotti, and D. S. Wiersma, Nature (London) **453**, 495 (2008).
[20] A. A. Fernández-Marín, J. A. Méndez-Bermúdez, J. Carbonell, F. Cervera, J. Sánchez-Dehesa, and V. A. Gopar, Phys. Rev. Lett. **113**, 233901 (2014).
[21] J. Klafter, M. F. Shlesinger, and G. Zumofen, Phys. Today **49**(2), 33 (1996).
[22] R. N. Mantegna and H. E. Stanley, Nature (London) **376**, 46 (1995).
[23] M. Leadbeater, V. I. Falko, and C. J. Lambert, Phys. Rev. Lett. **81**, 1274 (1998).
[24] H. Kohno and H. Yoshida, Solid State Commun. **132**, 59 (2004).
[25] D. W. Sims *et al.*, Nature (London) **451**, 1098 (2008).
[26] N. Mercadier, W. Guerin, M. Chevrollier, and R. Kaiser, Nat. Phys. **5**, 602 (2009).
[27] T. Holstein, Phys. Rev. **72**, 1212 (1947).
[28] J. P. Bouchaud and A. Georges, Phys. Rep. **195**, 127 (1990).
[29] P. Lévy, *Théorie de l'Addition des Variables Aléatoires* (Gauthiers-Villars, Paris, 1937).
[30] B. V. Gnedenko and A. N. Kolmogorov, *Limit Distributions for Sums of Independent Random Variables* (Addison-Wesley, Cambridge, 1954).
[31] V. V. Uchaikin and V. M. Zolotarev, *Chance and Stability: Stable Distributions and their Applications* (VSP, Utrecht, 1999), and references therein.
[32] F. Falceto and V. A. Gopar, Europhys. Lett. **92**, 57014 (2010).
[33] D. Boosé and J. M. Luck, J. Phys. A: Math. Theor. **40**, 14045 (2007).
[34] R. Burioni, L. Caniparoli, and A. Vezzani, Phys. Rev. E **81**, 060101(R) (2010).
[35] C. W. J. Beenakker, C. W. Groth, and A. R. Akhmerov, Phys. Rev. B **79**, 024204 (2009).
[36] R. T. Sibatov, JETP Lett. **93**, 503 (2011).
[37] P. W. Anderson, D. J. Thouless, E. Abrahams, and D. S. Fisher, Phys. Rev. B **22**, 3519 (1980).
[38] V. I. Mel'nikov, Pis'ma Zh. Eksp. Teor. Fiz. **32**, 244 (1980) [JETP Lett. **32**, 225 (1980)].
[39] A. A. Abrikosov, Solid State Commun. **37**, 997 (1981).
[40] P. A. Mello, J. Math. Phys. **27**, 2876 (1986).
[41] E. E. Kuruoğlu, IEEE Trans. Signal Process. **49**, 2192 (2001).

[42] P. A. Mello, P. Pereyra, and N. Kummar, Ann. Phys. (NY) **181**, 290 (1988).
[43] C. W. J. Beenakker and B. Rejaei, Phys. Rev. Lett. **71**, 3689 (1993).
[44] K. A. Muttalib, P. Wölfle, and V. A. Gopar, Ann. Phys. (NY) **308**, 156 (2003).
[45] V. A. Gopar, K. A. Muttalib, and P. Wölfle, Phys. Rev. B **66**, 174204 (2002).
[46] S. Datta, *Electronic Transport in Mesoscopic Systems* (Cambridge University Press, Cambridge, 1997).
[47] C. H. Lewenkopf and E. R. Mucciolo, J. Comput. Eletron. **12**, 203 (2013).